Applied Catalysis B: Environmental 197 (2016) 56–61

Contents lists available at ScienceDirect

Applied Catalysis B: Environmental

journal homepage: www.elsevier.com/locate/apcatb

Reconstruction of ceria-supported Pt-Co particles under H_2 and CO at 220 °C

D. Lorito[a], C. Ruocco[b], V. Palma[b], A. Giroir-Fendler[a], F.C. Meunier[a,*]

[a] Institut de Recherches sur la Catalyse et l'Environnement de Lyon, IRCELYON, Université Lyon 1, CNRS, Av. Albert Einstein, F-69626 Villeurbanne, France
[b] University of Salerno, Via Giovanni Paolo II, 132 84084 Fisciano, SA, Italy

ARTICLE INFO

Article history:
Received 27 November 2015
Received in revised form 11 January 2016
Accepted 14 January 2016
Available online 16 January 2016

Keywords:
Cobalt
Platinum
Ceria
CO hydrogenation
Fischer-Tropsch synthesis

ABSTRACT

Ceria-supported platinum and cobalt-based catalysts were investigated for the hydrogenation of CO at atmospheric pressure and 220 °C by operando diffuse reflectance FT-IR spectroscopy. The surface of $Pt/Co/CeO_2$ samples was constituted of alloyed phases following reduction at 450 °C. Cobalt-rich domains were then gradually formed under a CO/H_2 feed at 220 °C and atmospheric pressure. Pt-rich and Co-rich domains could be differentiated by the difference in reactivity of CO(ads) on the corresponding sites following CO removal from the feed. Pt is probably catalytically inactive under reaction condition, being poisoned by CO. Our data are consistent with Pt facilitating the dispersion and/or reduction of cobalt, although this could not be measured directly. The surface of ceria was initially covered with formates species that were gradually replaced with acetates, stressing the ability of ceria-promoted samples for improved oxygenate selectivity reported elsewhere.

1. Introduction

Cobalt-based catalysts are used for the production of synthetic fuels and base chemicals through the conversion of synthesis gas, a mixture of CO and H_2, via the Fisher-Tropsch process [1]. Platinum is sometimes used as a modifier of cobalt [1–5]. Pt is thought to facilitate the reduction of cobalt oxide precursors into the active phase metallic cobalt [2,3], although Tsubaki et al. proposed that the main role of Pt was to improve cobalt dispersion [6]. Jacobs et al. investigated ceria-supported Pt-Co particles for Fisher-Tropsch synthesis at 220 °C and 2 MPa and reported that the use of ceria as a support led to an increased proportion of oxygenates and linear alcohols as compared to the case of using alumina [3].

Platinum and cobalt in the metallic state form a solid solution, though ordering below 800 °C can occur leading to phases such as CoPt and $CoPt_3$ [7]. Dees and Ponec reported that bulk Pt-Co alloyed phases were observed for different Pt/Co ratios on silica-supported materials, but also suggested that the metal surface of bimetallic Pt/Co particles was enriched by cobalt [8]. Yet, no evidence of surface cobalt could be obtained using IR studies based on the adsorption of carbon monoxide, which is a standard molecular probe used to study metal surfaces. This fact might have actually been the result of the segregation that can occur in the presence of CO, leading to the preferential migration of Pt to the surface due to the formation of the stronger Pt-CO as compared to Co-CO, as proposed by Arenz and co-workers [9]. Similar observations have been made in the case of Pd-Au particles: Pd, which strongly binds CO contrary to Au, segregated towards the surface by CO [10].

Surface segregation in the presence of adsorbates such as O_2, H_2 or CO has in fact been often reported in the case of bimetallics [11]. Menning and Chen studied extended metallic surfaces based on Pt and Co and proposed that the surface was constituted of a Pt layer in vacuum or the presence of H_2, while a Co layer were present at the surface under O_2 [12]. Papaefthimiou et al. obtained similar results in the case of Pt-Co foils, yet stressing that several nanometer-thick cobalt oxide layers could be obtained under O_2 [13]. These authors also emphasised that the case of supported nanoparticles was more complex, as incomplete cobalt oxidation and reduction were observed under O_2 and H_2, respectively [13].

Jacobs et al. investigated the structure of alumina-supported Pt-Co particles by EXAFS and suggested that Pt was located on the edges of the particles and that reduction occurred on Pt first, allowing hydrogen to spill over to cobalt oxide and nucleate cobalt metal sites [2]. The presence of Pt enabled a more complete reduction of the cobalt oxide, though some cobalt aluminate remained. The Pt concentration used (Pt:Co atomic ratio <1/30) was much lower than that reported in most model studies, often using equimolar proportion of Co and Pt. Full external coverage of the particles by Pt atoms

* Corresponding author.
E-mail address: fcm@ircelyon.univ-lyon1.fr (F.C. Meunier).

http://dx.doi.org/10.1016/j.apcatb.2016.01.037
0926-3373/

may thereby impossible simply due to the limited availability of Pt atoms in each particle.

Wang et al. prepared Pt/Co colloidal particles (Pt:Co = 1/9 at.) and observed by atomic-resolution scanning transmission electron microscopy (STEM) a large variety of compositions, from pure Pt or Co to bimetallic particles [5]. All the reports discussed above indicate that the structure of Pt-Co particles are complex and may evolve depending on the reaction conditions. These observations stress the need to use of *in situ* techniques to investigate the sample structure under realistic operating conditions.

Several studies have reported *in situ* and *operando* FT-IR data of cobalt-based catalysts exposed to CO, the nature of the IR signal of CO(ads) and the corresponding adsorption sites being quite complex to unravel [14–17]. Surface reconstruction and roughening has been suggested to be facilitated by labile sub-carbonyl species Co-(CO) x, x = 1–4 [18] and the deposition of carbon [19]. Couble and Bianchi [20,21] showed that CO adsorbed on metallic cobalt lead to a band located at ca. 2030 cm^{-1}, yet the dissociation of CO readily led to the formation of a carbide phase, which resulted in the CO(ads) band shifting to ca. 2060 cm^{-1}. This transformation is yet readily reversible if H_2 is introduced in the feed. Paredes-Nunez et al. [22] confirmed these observations by *operando* diffuse reflectance FT-IR spectroscopy (DRIFTS) carried out at a temperature of 220 °C, which is typically used for Fischer-Tropsch synthesis over cobalt-based catalysts. It was also reemphasised that the cobalt surface reconstructs at atmospheric pressure under H_2/CO over a period of several hours [22].

There has been very few work dealing with in situ IR analyses of CO hydrogenation over Pt-Co-based catalysts [23] and none using ceria as a support. The aim of the present work was to study ceria-supported Pt-Co nanoparticles under a CO/H_2 feed and understand the nature of the surface and adsorbates that are present under reaction conditions at atmospheric pressure.

2. Experimental

Ceria was supplied by Sigma-Aldrich (nanopowder, particle size <25 nm, BET surface area of 80 $m^2\,g^{-1}$). The surface area of ceria support dropped to 60 $m^2\,g^{-1}$ following calcination at 600 °C for 3 h. The catalysts were prepared by wet impregnation using platinum tetrachloride (supplied by Strem Chemicals) and cobalt acetate tetrahydrate (supplied by Sigma Aldrich) as precursors. The required amount of precursors were dissoluted in 500 ml of distilled water at ambient conditions. The resulting slurry was stirred on a heating plate (T = 250 °C) until water evaporated. The samples were then dried at 120 °C overnight and eventually calcined in ambient air at 600 °C for 3 h (ramp 10 °C/min). The Co and Pt deposition was obtained by two successive impregnations, Co first followed by that of Pt [24]. The measured loadings of Co and Pt were essentially identical to the nominal values and the BET surface areas of the samples were around 40 $m^2\,g^{-1}$. (Table S1, Supplementary information).

DRIFTS experiments were performed at ambient pressure with a high temperature DRIFT cell (from Spectra-Tech®) fitted with KBr windows, using a collector assembly. A description and properties of the cell can be found elsewhere [25]. High purity Ar, CO and H_2 were purchased from l'Air Liquide. The gases were used without further purification.

The spectrophotometer used was a Nicolet 6700 (ThermoFischer Scientific) fitted with a liquid-N_2 cooled MCT detector. The DRIFT spectra were recorded at a resolution of 4 cm^{-1} and 8 or 32 scans accumulation depending on the time-resolution desired. The DRIFTS spectra are reported as log (1/R), where R is the sample reflectance. This pseudo-absorbance gives a better linear representation of the band intensity against surface coverage than that given by the Kubelka-Munk function for strongly absorbing media such as those based on metals supported on oxides [26]. The contribution of gas-phase CO was subtracted using a CO(g) spectrum collected at the reaction temperature over SiC, which enabled a correction that did not distort the baseline [27].

The catalysts were pre-reduced at 450 °C for 1 h in a flow of 55 STPmL min^{-1} of 60% H_2 in Ar. The samples were then cooled to the reaction temperature. The feed composition was: 30% CO + 60% H_2 in Ar, unless otherwise stated. The total flow rate was 30 ml min^{-1}, unless otherwise stated. The gas hourly space velocity (GHSV) was about 18000 h^{-1}. The CO conversion was always lower than 3% and therefore the DRIFTS cell could be considered as a differential reactor.

The reactor effluent was analysed both using an Inficon quadrupolar mass spectrometer and a FT-IR gas-cell fitted in a Nicolet spectrometer. The IR gas-cell exhibited a 2 m-long pathlength and enabled measuring concentration of reaction products in the tens of ppm. Several m/z fragments were recorded over the mass spectrometer over the 2–80 m/z range.

3. Results

3.1. Catalytic activity

The samples were pre-treated under H_2 at 450 °C for 60 min to reduce part of the cobalt oxide into a metallic state. The extent of cobalt reduction was not assessed *in situ*, but alumina-supported cobalt samples (non-promoted by a noble metal) reduced under similar conditions would typically display a level of reduction comprised between 60 and 80% [28–31]. The activity pattern was similar over the Co/CeO_2 and the two Pt-promoted samples (Fig. 1). Note that these samples were about one order of magnitude less active than alumina-supported samples measured under identical conditions in the same DRIFTS cell [22,32,33].

The main reaction product was methane, followed by propene, ethene and methanol. The rate of formation of these products was essentially constant with time, apart from a deactivation occurring in the first few hours on stream. The sharp methane decay in methane production observed initially is related to the fact that the reduced cobalt surface is only covered with hydrogen, leading to a fast methane production once CO is introduced. The rate of methane formation subsequently decreases as the cobalt surface because covered (poisoned) by CO. Such methane spikes are observed whenever CO is added or removed from the feed [17].

The rates of product formation at pseudo-steady-state (*i.e.* after 23 h on stream) are shown in Fig. 2. The addition of platinum led to a minor improvement in the rate of methane formation, while a minor decrease of propene and ethene formation. The effect of platinum was stronger in the case of methanol formation.

The corresponding concentrations were minute, ca. 41, 2.4, 4.3 and 6.9 ppm for methane, ethene, propene, and methanol, respectively, over the 3% Pt/10% Co/CeO_2. Propene was more abundant than ethene as typically observed in product distributions of Fischer-Tropsch syntheses under similar conditions [34]. The product distribution pattern observed here is consistent with that reported by Shi et al. over a cobalt-based sample [35]. The carbon balance could not be established accurately, because the CO conversion was too low and the relative error on product selectivity too important. Ethanol could not be observed under these conditions.

3.2. Operando diffuse reflectance FT-IR spectra

The *operando* DRIFTS spectra collected over the Co/CeO_2 sample and the two Pt-promoted catalysts at various times on stream are shown in Fig. 3. The absolute absorbance of bands cannot be

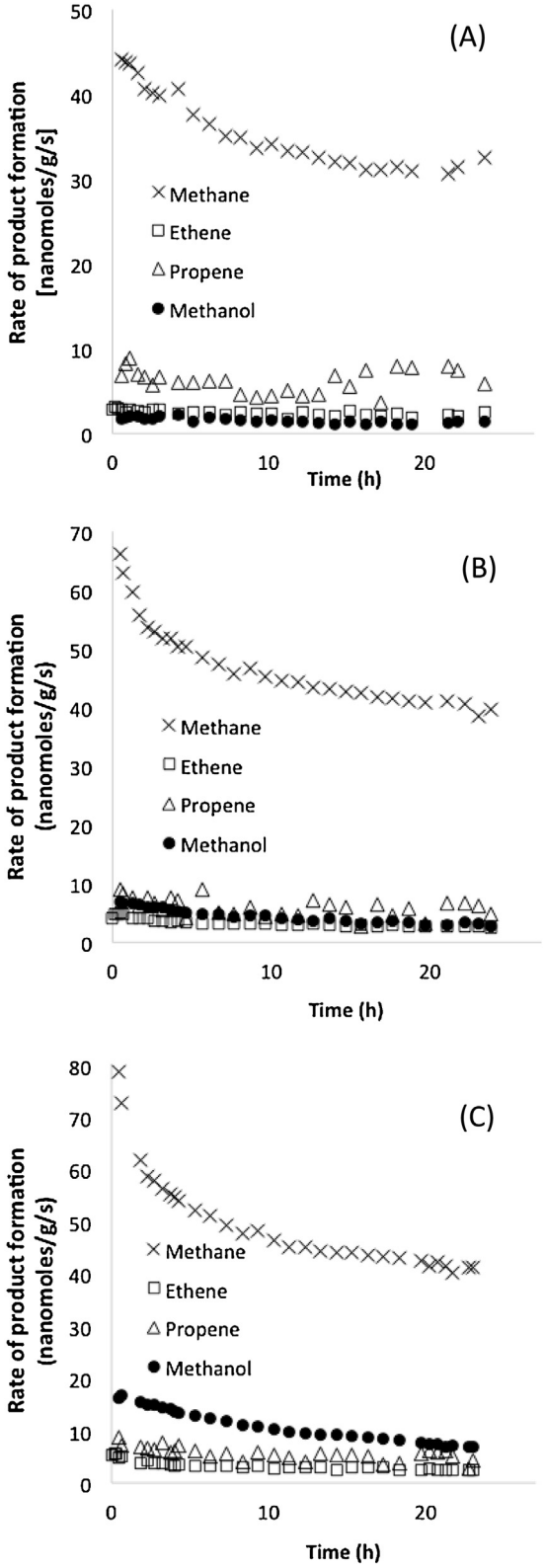

Fig. 1. Rates of formation of methane, ethene, propene and methanol over the various catalysts at 220 °C at steady-state over 23 h under 30% CO + 60% H_2: (A) 10% Co/CeO_2, (B) 0.4% Pt/10% Co/CeO_2 and (C) 3% Pt/10% Co/CeO_2.

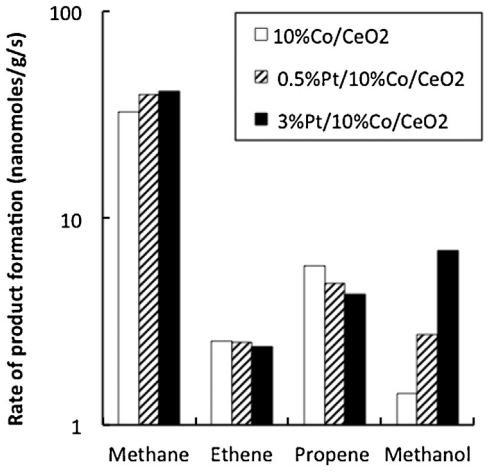

Fig. 2. Comparison of the rates of formation of methane, ethene, propene and methanol over the various catalysts at 220 °C at steady-state after 23 h under 30% CO + 60% H_2.

Table 1
Bands observed on the catalysts during DRIFTS experiments and the corresponding surface species and vibrations to which they were assigned. (s = symmetric, a = asymmetric, ν = stretching, δ = bending).

Wavenumber/cm-1	Surface species	Vibration	References
2034–2025	Linear CO on cobalt	ν_{CO}	[20–22]
2065–2058	Linear CO on platinum	ν_{CO}	[36,37]
1950–1650 cm^{-1}	Bridged and multi-bonded CO on cobalt	ν_{CO}	[20,21,33]
1562–1555	Acetate CH_3COO_{OCO}	$\nu^a{}_{OCO}$	[40–42]
1427–1425		$\nu^s{}_{OCO}$	
2845	Formate $HCOO_{CH}$	ν_{CH}	[38–41]
1575–1570		$\nu^a{}_{OCO}$	
1370		δCH	
1335		νsOCO	
2925, 2850	—CH_2— of alkanes	ν_{CH}	[22]
1612, 1300	Carbonates		[40]

directly compared, because the IR optical pathway can be different for each sample depending on the sample absorptivity (which depends, among others, on the metal content, level of reduction and particle sizes). Only the band position (Table 1) and relative intensity should therefore be discussed.

A band located at 2034 cm^{-1} typical of CO linearly adsorbed on metallic cobalt can be observed on the Co/CeO_2. The band gradually shifted to 2025 cm^{-1} with time. A similar behavior was noted over alumina-supported cobalt [22], which was suggested to be related to surface restructuring [18,19]. A very broad band also developed over the 1950–1650 cm^{-1} range, indicating the presence of bridged and multi-bonded CO [20,21,33].

The spectra obtained over the Pt-promoted samples showed marked differences. A sharp carbonyl band at ca. 2060 cm^{-1} was noted at all times, associated with CO linearly adsorbed on Pt [36,37]. The evolution of the CO(ads) band in the case of the 3% Pt/10% Co/CeO_2 is shown in detail in Fig. 4. Only the Pt carbonyl band at 2065 cm^{-1} was resolved in the first minute on stream. The band was broad and asymmetric, so the overall signal likely comprised many other bands.

A second band became gradually resolved at 2044 cm^{-1} after 2 h and was shifted to 2034 cm^{-1} after 24 h. The signal in the region 1950–1650 cm^{-1} markedly increased (see shift with respect the baseline level at 2100 cm^{-1}), similarly to the case of the Pt-free sample, although no resolved band could be observed. These newly formed bands were likely related to CO adsorbed on cobalt atoms or Pt-Co phases.

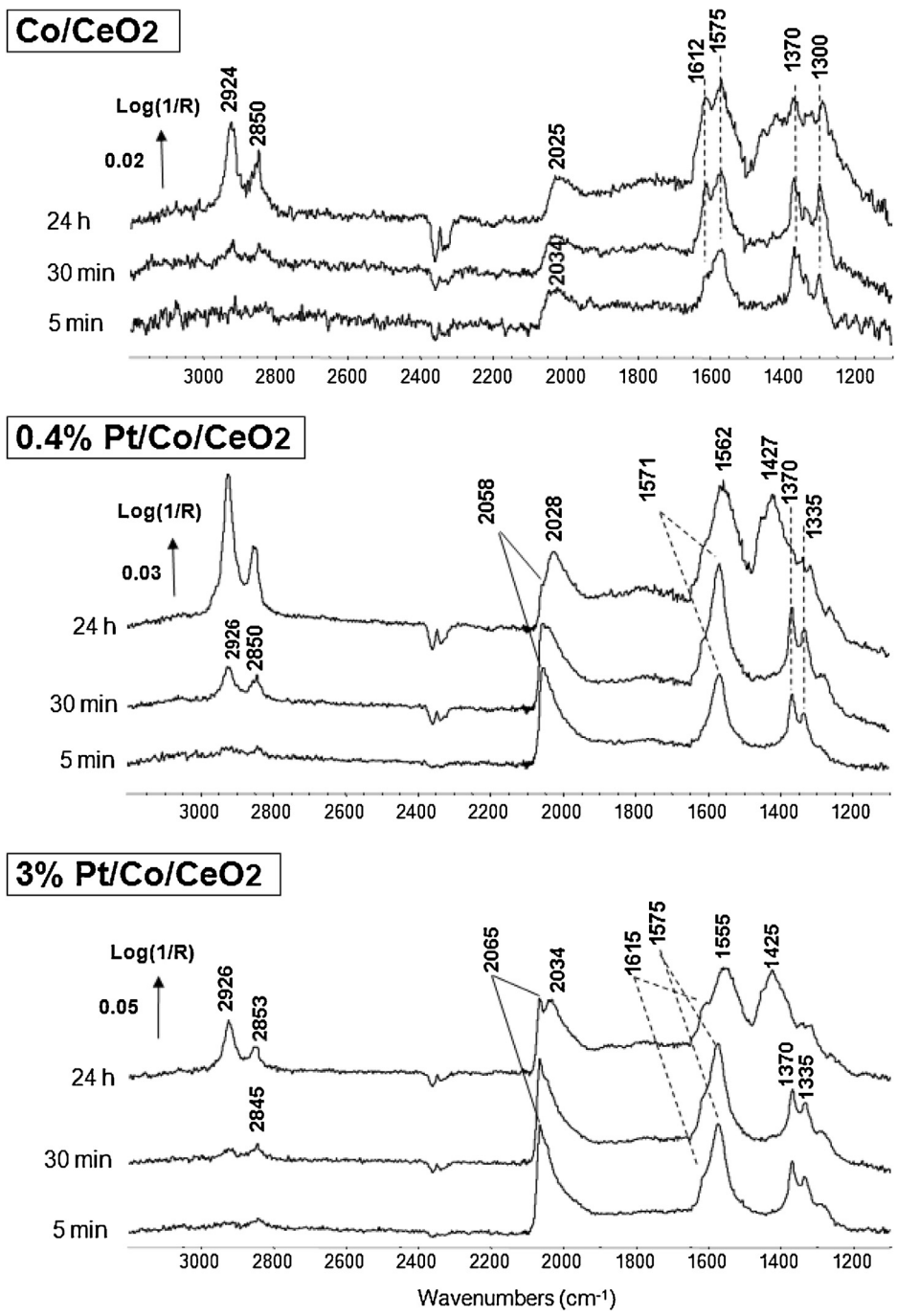

Fig. 3. *Operando* DRIFTS spectra collected at 220 °C at various time on stream over the CeO2-based catalysts. Feed: 30% CO + 60% H_2 in Ar. The signal of the sample at the corresponding temperature under H_2 was used as background. The spectrum of CO(g) was subtracted.

Several sharp bands could be observed below 1650 cm^{-1}. The set of bands at ca. 2845, 1575, 1370 and 1335 cm^{-1} that were especially visible at 5 and 30 min can be assigned to formate species formed on ceria [38–41]. The band at 1612 and 1300 cm^{-1} are possibly due to a carbonate or bicarbonate species [40,42]. The spectrum collected after 24 h exhibited bands at ca. 2925 and 2850 cm^{-1}, which were barely visible after 30 min on stream. These bands are associated with the stretching vibration of methylene groups (-CH_2-), typical of long carbon chain alkanes, which may accumulate in the catalyst pores [22].

The spectrum in the 1650–1200 cm^{-1} region after 24 h for the Pt-free sample was poorly resolved and corresponded to the superimposition of several bands related to formates, acetates (ca. 1560 and 1425 cm^{-1} [40–42]) and various bending modes associated with alkanes. In contrast, this spectral region showed mostly acetate bands in the case of the Pt-promoted sample after 24 h, while the bands associated with formates had sharply decreased in intensity.

3.3. Reactivity of the carbonyl surface species

The spectra reported in Figs. 3 and 4 showed that the CO(ads) signal was quite complex and evolved with time. A experiment consisting in removing CO from the feed was carried out to better understand the nature and reactivity of the CO(ads) present

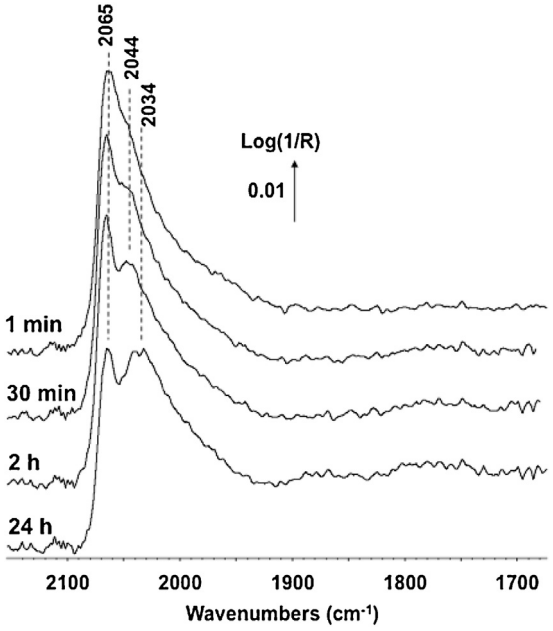

Fig. 4. *Operando* DRIFTS spectra collected at 220 °C at various time on stream over the 3% Pt/10%Co/CeO_2. Feed: 30% CO + 60% H_2 in Ar. The signal of the sample at the corresponding temperature under H_2 was used as background. The spectrum of CO(g) was subtracted.

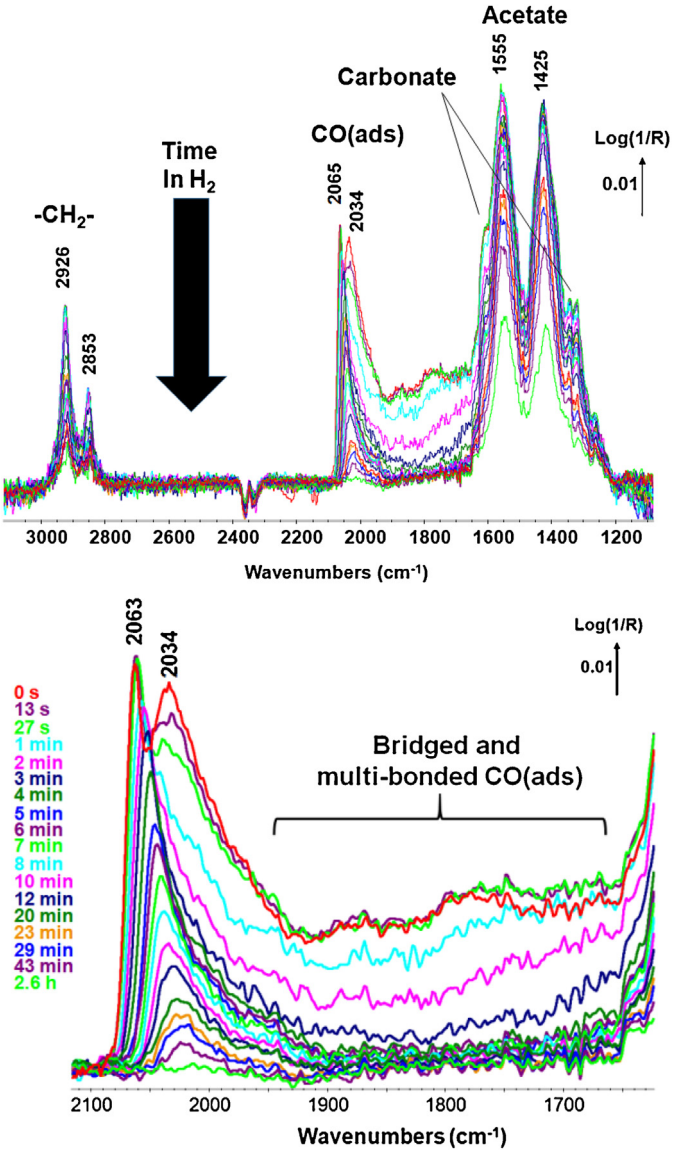

Fig. 5. *in situ* DRIFTS spectra collected at 220 °C at various time on stream over the 3% Pt/10%Co/CeO_2 following the removal of 30% CO at time = 0. Feed: 60% H_2 in Ar. The signal of the sample at the corresponding temperature under H_2 was used as background. The bottom figure is a magnification on the CO(ads) region of the top figure, also showing the legend.

at 220 °C in the presence of H_2. The data relating to the 3% Pt/10%Co/CeO_2 are shown in Fig. 5 over a period of 2.6 h.

The IR bands associated with alkanes, CO(ads), carbonate and acetate species gradually decreased with time under H_2, as a result of adsorbate desorption and/or conversion. The decay of the carbonyl signal was not uniform (Fig. 5, bottom). The band assigned to CO adsorbed on Pt at ca. 2063 cm^{-1} decreased markedly slower than that related to cobalt at 2034 cm^{-1}. The decay of the unresolved broad bands of bridged/multibonded CO(ads) comprised between 1950 and 1650 cm^{-1} was as fast as that of the 2034 cm^{-1} cobalt band, which had both vanished after about 4 min. In contrast, the Pt-CO band was still present after 40 min.

Ex situ TEM analyses (Fig. S1 and S2, Supplementary information) revealed the presence of a few large Pt-rich particles (almost with no cobalt) up to 100 nm in size, while most of the sample appeared to consist of particles with a size centered around 20 nm and containing both metals. It is therefore clear that particle size and composition varied, though it is difficult to determine the exact distribution due to the poor contrast obtained by TEM over this type of material. The approximate metal dispersion was about 5%. Since the molar proportion Pt was ca. 7% with respect to all (Pt + Co) in the 3% Pt/10% Co/CeO_2, it is therefore theoretically possible for this sample that the metallic surface could have been fully covered with Pt atoms.

4. Discussion

The data reported here show that the structure of Pt-Co particles obtained by successive impregnation, calcinations and reduction is complex. Heterogeneity in size and composition make any global evaluation difficult. Yet, important conclusions can be drawn on the activity and stability of Pt-Co particles under the conditions of pressure and temperature used here, which are partly relevant to Fischer-Tropsch synthesis.

The rather similar activity (both in terms of magnitude and evolution with time) of the Pt-promoted samples and that free of Pt (Figs. 1 and 2) indicates that similar concentrations of cobalt atoms were present on the various samples, as Pt is poorly active for CO hydrogenation under these conditions [43]. The higher rate of methane formation observed at short time on stream was likely due to a promoting effect of "clean" Pt able to activate H_2, before this metal eventually became poisoned.

The minor increase and decrease in methane and propene formation, respectively, observed at pseudo-stady-state (*i.e.* after 24 h) over the Pt-modified samples could possibly be an indirect effect of an increased cobalt dispersion and/or reduction due to the presence of Pt, as proposed by other authors [2,3,6]. Smaller cobalt particles are indeed more selective for methane formation [44].

The increased production of methanol due to Pt (Figs. 1 and 2) might also be due to an increase dispersion of cobalt, since it was recently proposed that methanol was formed by hydrogenation of formates located at the interface of cobalt and the alumina support [32]. The larger activity change observed for methanol as compared to the cases of methane and propene arises from the different mechanism and sites involved [32].

Ceria appeared yet to lead to a different surface chemistry as compared to the case of alumina-supported cobalt. The main IR bands over alumina-supported cobalt catalysts used under similar conditions were and always remained those of formates [22,32]. In contrast, the surface of ceria, promoted or not by Pt, got gradually covered with other oxygenated species, in particular acetates (Fig. 3). This was likely due to the redox properties of ceria, which is known to facilitate adsorbate oxidation as reported by Idriss et al. [42] and explain the improved oxygenate selectivity reported by Davis and co-workers over Pt-Co/CeO_2 catalysts used for Fisher-Tropsch synthesis [3].

The IR data shown in Figs. 3 and 4 indicate that the state of the surface of the Pt-containing samples at 220 °C under CO/H_2 following reduction with H_2 at 450 °C is initially quite different from that corresponding to the Pt-free sample. The band of cobalt-adsorbed CO at ca. 2030 cm^{-1} was initially not visible and could only be resolved after a few hours on stream. Since the concentration of surface cobalt was expected to remain similar (*vide supra*), it must be concluded that the state of the cobalt sites were markedly different. This can be rationalised by proposing that an alloyed phase was initially present, which subsequently gradually segregated.

It is yet impossible for us to determine whether or not Pt was still present within Co phases after 24 h on stream, though Pt was likely decorating some sites on cobalt domains, as proposed by Jacobs et al. based *on in situ* EXAFS data [2]. It is also difficult to determine from our IR data whether or not any surface segregation of Pt occurred during this restructuring, due to the complexity of the decomposition of IR bands of CO adsorbed on metals [45–47].

The IR signal of CO adsorbed on metal sites could yet be parted into two main contributions by following signal decay upon CO removal (Fig. 5). One contribution was Co-rich, related to the most reactive bands at 2030 cm^{-1} and those between 1950 and 1650 cm^{-1}. The other one was associated with Pt-rich phase (band at 2063 cm^{-1}), which slowly vanished under a CO-free feed. The data suggest that under CO/H_2 feed at 220 °C, a temperature typically used for Fischer-Tropsch synthesis over cobalt-based catalysts, the Pt is essentially poisoned by CO and plays very little direct catalytic role, if any at all. Pt is of course crucial at higher temperatures in the absence of CO, as used during sample reduction.

5. Conclusions

The surface of Pt/Co/CeO_2 samples is composed alloyed phases following reduction at 450 °C. Cobalt-rich domains are then gradually formed under a CO/H_2 feed at 220 °C and atmospheric pressure. Pt is probably inactive under reaction condition, being poisoned by CO. Our data are consistent with Pt facilitating the dispersion and/or reduction of cobalt, although this could not be measured directly. The surface of ceria is initially covered with formates species that are gradually replaced with acetates, stressing the ability of ceria-promoted sample for improved oxygenate selectivity observed elsewhere.

Acknowledgment

D.L. acknowledges a PhD scholarship from the Ministry of higher Education and Research of France at the University of Lyon.

Appendix A. Supplementary data

Supplementary data associated with this article can be found, in the online version, at http://dx.doi.org/10.1016/j.apcatb.2016.01.037.

References

[1] A.Y. Khodakov, W. Chu, P. Fongarland, Chem. Rev. 107 (2007) 1692–1744.
[2] G. Jacobs, J.A. Chaney, P.M. Patterson, T.K. Das, J.C. Maillot, B.H. Davis, J. Synchrotron Radiat. 11 (2004) 414.
[3] M.K. Gnanamani, M.C. Ribeiro, W. Ma, W.D. Shafer, G. Jacobs, U.M. Graham, B.H. Davis, Appl. Catal. A: Gen. 393 (2011) 17–23.
[4] D.O. Silva, L. Luza, A. Gual, D.L. Baptista, F. Bernardi, J.M. Zapata, J. Morais, J. Dupont, Nanoscale 6 (2014) 9085–9092.
[5] H. Wang, W. Zhou, J.-X. Liu, R. Si, G. Sun, M.-Q. Zhong, H.-Y. Su, H.-B. Zhao, J.A. Rodriguez, S.J. Pennycook, J.-C. Idrobo, W.-X. Li, Y. Kou, D. Ma, J. Am. Chem. Soc. 135 (2013) 4149–4158.
[6] N. Tsubaki, S.L. Sun, K. Fujimoto, J. Catal. 199 (2001) 236–246.
[7] A.S. Darling, Platinum Metals Rev. 7 (1963) 96–104.
[8] M.J. Dees, V. Ponec, J. Catal. 119 (1989) 376.
[9] K.J.J. Mayrhofer, V. Juhart, K. Hartl, M. Hanzlik, M. Arenz, Angew. Chem. Int. Ed. 48 (2009) 3529–3531.
[10] L. Delannoy, S. Giorgio, J.G. Mattei, C.R. Henry, N. El Kolli, C. Méthievier, C. Louis, ChemCatChem 5 (2013) 2707–2716.
[11] S. Zafeiratos, S. Piccinin, D. Teschner, Catal. Sci. Technol. 2 (2012) 1787–1801.
[12] C.A. Menning, J.G. Chen, J. Power Sources 195 (2010) 3140–3144.
[13] V. Papaefthimiou, T. Dintzer, V. Dupuis, A. Tamion, F. Tournus, D. Teschner, M. Haevecker, A. Knop-Gericke, R. Schloegl, S. Zafeiratos, J. Phys. Chem. Lett. 2 (2011) 900–904.
[14] G.A. Beitel, A. Laskov, H. Oosterbeek, E.W. Kuipers, J. Phys. Chem. 100 (1996) 12494–12502.
[15] D. Song, J. Li, Q. Cai, J. Phys. Chem. C 111 (2007) 18970–18979.
[16] U. Cornaro, S. Rossini, T. Montanari, E. Finocchio, G. Busca, Catal. Today 197 (2012) 101–108.
[17] J. Schweicher, A. Frennet, N. Kruse, H. Daly, F.C. Meunier, J. Phys. Chem. C 114 (2010) 2248–2255.
[18] J. Wilson, C. de Groot, J. Phys. Chem. 99 (1995) 7860–7866.
[19] C.J. Weststrate, I.M. Ciobîca, A.M. Saib, D.J. Moodley, J.W. Niemantsverdriet, Catal. Today 228 (2014) 106–112.
[20] J. Couble, D. Bianchi, J. Phys. Chem. C 117 (2013) 14544–14557.
[21] J. Couble, D. Bianchi, Appl. Catal. A: Gen. 445446 (2012) 1–13.
[22] A. Paredes-Nunez, D. Lorito, N. Guilhaume, C. Mirodatos, Y. Schuurman, F.C. Meunier, Catal. Today 242 (2015) 178–183.
[23] M. Kollár, A. De Stefanis, H.E. Solt, M.R. Mihályi, J. Valyon, A.A.G. Tomlinson, J. Mol. Catal. A: Chem. 333 (2010) 37–45.
[24] V. Palma, F. Castaldo, P. Ciambelli, G. Iaquaniello, G. Capitani, Int. J. Hydrogen Energy 38 (2013) 6633–6645.
[25] H. Li, M. Rivallan, F. Thibault-Starzyk, A. Travert, F.C. Meunier, Phys. Chem. Chem. Phys. 15 (2013) 7321–7327.
[26] J. Sirita, S. Phanichphant, F.C. Meunier, Anal. Chem. 79 (2007) 3912–3918.
[27] A. Paredes-Nunez, I. Jbir, D. Bianchi, F.C. Meunier, Appl. Catal. A: Gen. 315 (2015) 17–22.
[28] R. Bechara, D. Balloy, J.-Y. Dauphin, J. Grimblot, Chem. Mater. 11 (1999) 1703–1711.
[29] W.-J. Wang, Y.-W. Chen, Appl. Catal. 77 (1991) 223–233.
[30] S. Storsæter, B. Tøtdal, J.C. Walmsley, B. Steinar Tanem, A. Holmen, J. Catal. 236 (2005) 139–152.
[31] A. Lapidus, A. Krylova, V. Kazanskii, V. Borovkov, A. Zaitzev, J. Rathousky, A. Zukal, M. Jancalkova, Appl. Catal. 73 (1991) 65–82.
[32] D. Lorito, A. Paredes-Nunez, C. Mirodatos, Y. Schuurman, F.C. Meunier, Catal. Today 259 (2015) 192–196.
[33] A. Paredes-Nunez, D. Lorito, Y. Schuurman, N. Guilhaume, F.C. Meunier, J. Catal. 329 (2015) 229–236.
[34] J. Cheng, P. Hu, P. Hellis, S. French, G. Kelly, C.M. Lok, J. Catal. 257 (2008) 221–228.
[35] L. Shi, C. Zeng, Q. Lin, W. Niu, N. Tsubaki, Catal. Today 228 (2014) 206–211.
[36] A. Goguet, F.C. Meunier, D. Tibiletti, J.P. Breen, R. Burch, J. Phys. Chem. B 108 (2004) 20240–20246.
[37] A. Moscu, Y. Schuurman, L. Veyre, C. Thieuleux, F.C. Meunier, Chem. Commun. 50 (2014) 8590–8592.
[38] G. Busca, J. Lamotte, J.C. Lavalley, V. Lorenzelli, J. Am. Chem. Soc. 109 (1987) 5197–5202.
[39] C. Li, K. Domen, K.-I.M.T. Onishi, J. Catal. 125 (1990) 445–455.
[40] C. Binet, M. Daturi, J.-C. Lavalley, Catal. Today 50 (1999) 207–225.
[41] M. Li, Z. Wu, S.H. Overbury, J. Catal. 306 (2013) 164–176.
[42] A. Yee, S.J. Morrison, H. Idriss, J. Catal. 186 (1999) 279–295.
[43] P. Panagiotopoulou, D.I. Kondarides, X.E. Verykios, Appl. Catal. A: Gen. 344 (2009) 45–54.
[44] G.L. Bezemer, J.H. Bitter, H.P.C.E. Kuipers, H. Oosterbeek, J.E. Holewijn, X. Xu, F. Kapteijn, A.J. van Dillen, K.P. de Jong, J. Am. Chem. Soc. 128 (2006) 3956–3964.
[45] V.M. Browne, S.G. Fox, P. Hollins, Catal. Today 9 (1991) 1–14.
[46] V.M. Browne, S.G. Fox, P. Hollins, Mater. Chem. Phys. 29 (1991) 235–244.
[47] S.G. Fox, V.M. Browne, P. Hollins, J. Electron Spectrosc. Relat. Phenom. 54/55 (1990) 749–758.